Journal of Orthopaedic Translation 41 (2023) 33–41

Contents lists available at ScienceDirect

Journal of Orthopaedic Translation

journal homepage: www.journals.elsevier.com/journal-of-orthopaedic-translation

Disruption of Col9a2 expression leads to defects in osteochondral homeostasis and osteoarthritis-like phenotype in mice

Rui Dong [a,b,1], Huihui Xu [a,c,1], Pinger Wang [a,c], Liang Fang [a,c], Luwei Xiao [b,c], Shuaijie Lv [a,b,**], Peijian Tong [a,b,***], Hongting Jin [a,c,*]

[a] Institute of Orthopaedics and Traumatology of Zhejiang Province, The First Affiliated Hospital of Zhejiang Chinese Medical University (Zhejiang Provincial Hospital of Chinese Medicine), No.548, Binwen Road, Hangzhou, Zhejiang, 310053, PR China
[b] Department of Orthopaedic Surgery, The First Affiliated Hospital of Zhejiang Chinese Medical University (Zhejiang Provincial Hospital of Chinese Medicine), No.54, Youdian Road, Hangzhou, Zhejiang, 310006, PR China
[c] Department of Orthopaedic Surgery, The First Affiliated Hospital of Zhejiang Chinese Medical University (Zhejiang Provincial Hospital of Chinese Medicine), No.54, Youdian Road, Hangzhou, Zhejiang Province, 310006, PR China

ARTICLE INFO

Keywords:
Col9a2
Osteochondral
Homeostasis
Knee osteoarthritis

ABSTRACT

Background/Objective: As one of the branched chains of Type IX collagen (Col9), Collagen IX alpha2 (Col9a2) has been reported to be associated with several orthopedic conditions. However, the relationship between Col9a2 and knee osteoarthritis (KOA) remains to be elucidated.

Methods: To probe the relationship between Col9a2 and KOA, we performed a systematic analysis of Col9a2-deficient ($Col9a2^{-/-}$) mice using whole-mount skeletal staining, Micro-CT (μCT), biomechanics, histomorphometry, immunohistochemistry (IHC), immunofluorescence (IF) and Elisa.

Results: We found that the subchondral bone (SCB) in the knee joint of $Col9a2^{-/-}$ mice became sparse and deformed in the early stage, with altered bone morphometric parameters, reduced load-bearing capacity, dysfunctional bone homeostasis (decreased osteogenesis capacity and elevated bone resorption capacity), diminished cartilage proteoglycans and disrupted cartilage extracellular matrix (ECM) anabolism and catabolism compared with the $Col9a2^{+/+}$ mice. In the late stage, the cartilage degeneration in $Col9a2^{-/-}$ mice were particularly pronounced compared to $Col9a2^{+/+}$ mice, as evidenced by severe cartilage destruction and a marked reduction in cartilage thickness and area.

Conclusion: Overall, Col9a2 is essential for maintaining osteochondral homeostasis in the knee joint of mice, and the absence of this gene is accompanied by distinct sclerosis of the SCB and a reduction in load-bearing capacity; in the late stage, in the lack of SCB stress inhibition, excessive load is consistently exerted on the cartilage, ultimately leading to osteoarthritic-like articular cartilage damage.

The translational potential of this article

This study highlights the critical importance of Col9a2 for maintaining osteochondral homeostasis in the knee joint of mice. Knockout of this gene resulted in osteoarthritis-like articular cartilage damage. Hence, Col9a2 may serve as a potential candidate biomarker associated with KOA.

1. Introduction

Type IX collagen (Col9) is heterotrimeric collagen consisting of three different α chains (α1, α2 and α3), expressed mainly in cartilage and found on the surface of tissues containing type II collagen (Col2), such as articular cartilage and vitreous humor [1,2]. As fiber-related collagen with an interrupted triple helix, Col9 assembles with Col2 to form heterogeneous fibers. It cross-links with Col2 located on the fibril surface, with its non-collagenous NC4 structural domain projecting outwards [3].

* Corresponding author. The First College of Clinical Medicine, Zhejiang Chinese Medical University, Hangzhou, 310053, Zhejiang Province, PR China.
** Corresponding author. The First College of Clinical Medicine, Zhejiang Chinese Medical University, Hangzhou, 310053, Zhejiang Province, PR China.
*** Corresponding author. The First College of Clinical Medicine, Zhejiang Chinese Medical University, Hangzhou, 310053, Zhejiang Province, PR China.
E-mail addresses: lvshuaijie1990@126.com (S. Lv), peijiantongzjtcm@163.com (P. Tong), hongtingjin@163.com (H. Jin).
[1] Contributed equally.

https://doi.org/10.1016/j.jot.2023.08.005
Received 25 May 2023; Received in revised form 14 July 2023; Accepted 2 August 2023

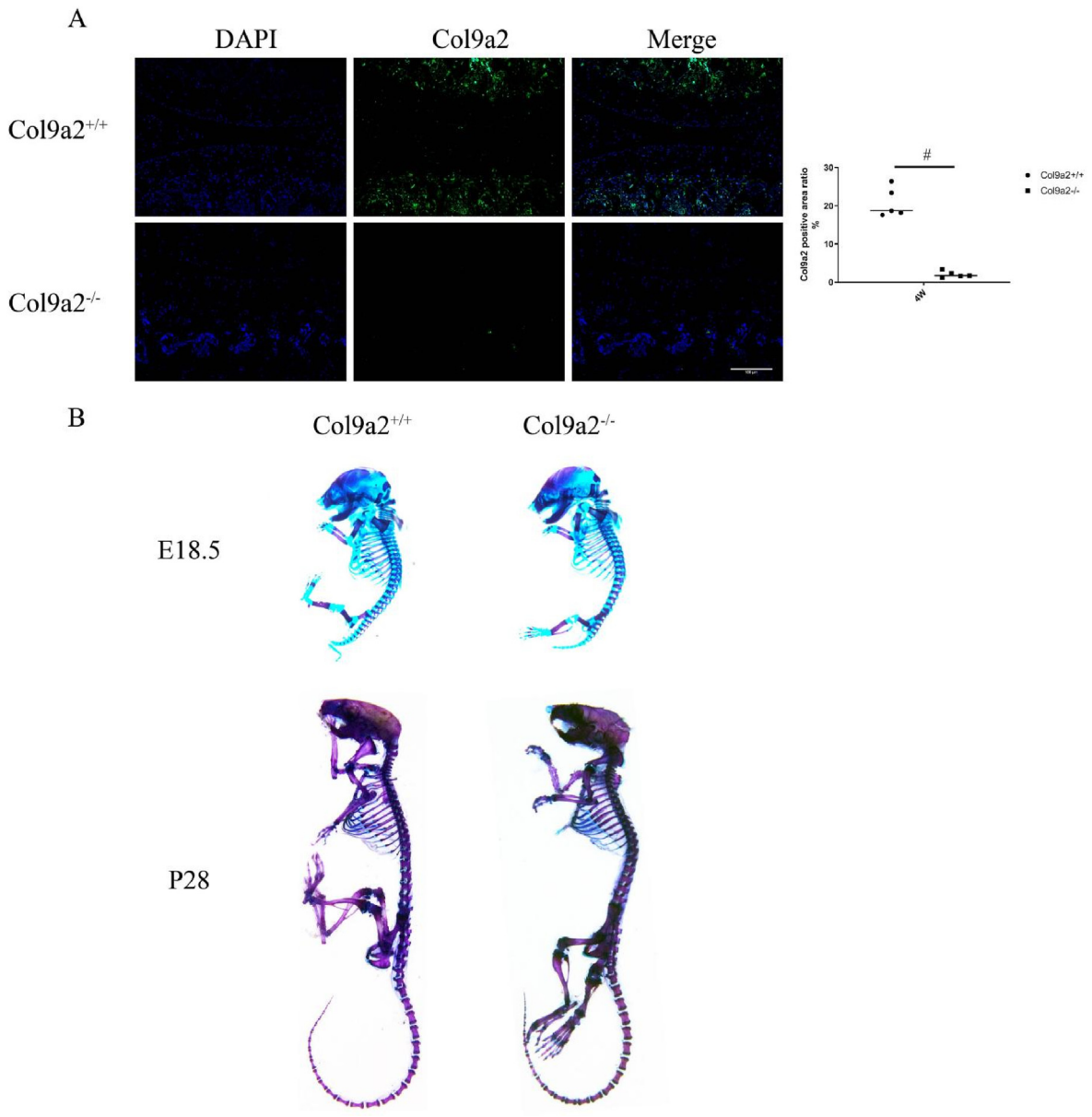

Figure 1. Immunofluorescence of Col9a2 and whole-mount skeletal staining of mice. A Immunofluorescence and quantitative analysis of Col9a2 in 4-week-old mice. Scale bar: 100 μm. B Whole-mount skeleton staining of embryos (E18.5) and adult mice (P28). All data were expressed as mean ± SD, $^{\#}P < 0.01$.

Multiple interactions with other cartilage matrix proteins have been assigned to this structural domain, suggesting that Col9 bridges the collagen network and other extracellular matrix (ECM) superstructures [4].

As an integral component of articular cartilage and bone matrix [5–7], polymorphisms in Col9 have been reported to be associated with several orthopedic conditions. As one of the branched chains of Col9, Collagen IX alpha2 (Col9a2) has been most frequently reported to be involved in lumbar disc degeneration [8–10] and lumbar spinal stenosis [6,11]. Our previous study has also demonstrated that the absence of Col9a2 leads to osteochondral remodeling of the cartilage endplate and inhibits ECM synthesis, which accelerates matrix degradation and chondrocyte hypertrophy in the intervertebral disc tissue [7]. However, some studies have also found a strong relationship between Col9a2 and the development of osteoarthritis (OA) of the hip [12] and multiple epiphyseal dysplasia [13,14].

A recent study suggested that Col9a2 may be a potential candidate biomarker associated with OA, based on a comprehensive systematic analysis that reported a positive relationship between Col9a2 and OA [15], and combined with the strong correlation of Col9a2 with orthopedic diseases, it is reasonable to speculate that deletion of the Col9a2 is also implicated in the development of knee osteoarthritis (KOA). What are the specific changes and the underlying mechanisms if this is the case? Therefore, based on the above hypothesis, the current study provides the first evidence for the contribution of Col9a2 to osteochondral homeostasis in the knee joint and further observed the correlation with time.

2. Materials and methods

2.1. Mice

Collagen IX alpha2-deficient ($Col9a2^{-/-}$) mice were constructed from the Nanjing Biomedical Research Institute of Nanjing University (Grade SPF II, XM002445). Briefly, chimeric mice ($Col9a2^{+/-}$) were generated and mated them for 10 generations. $Col9a2^{-/-}$ mice and their wild-type

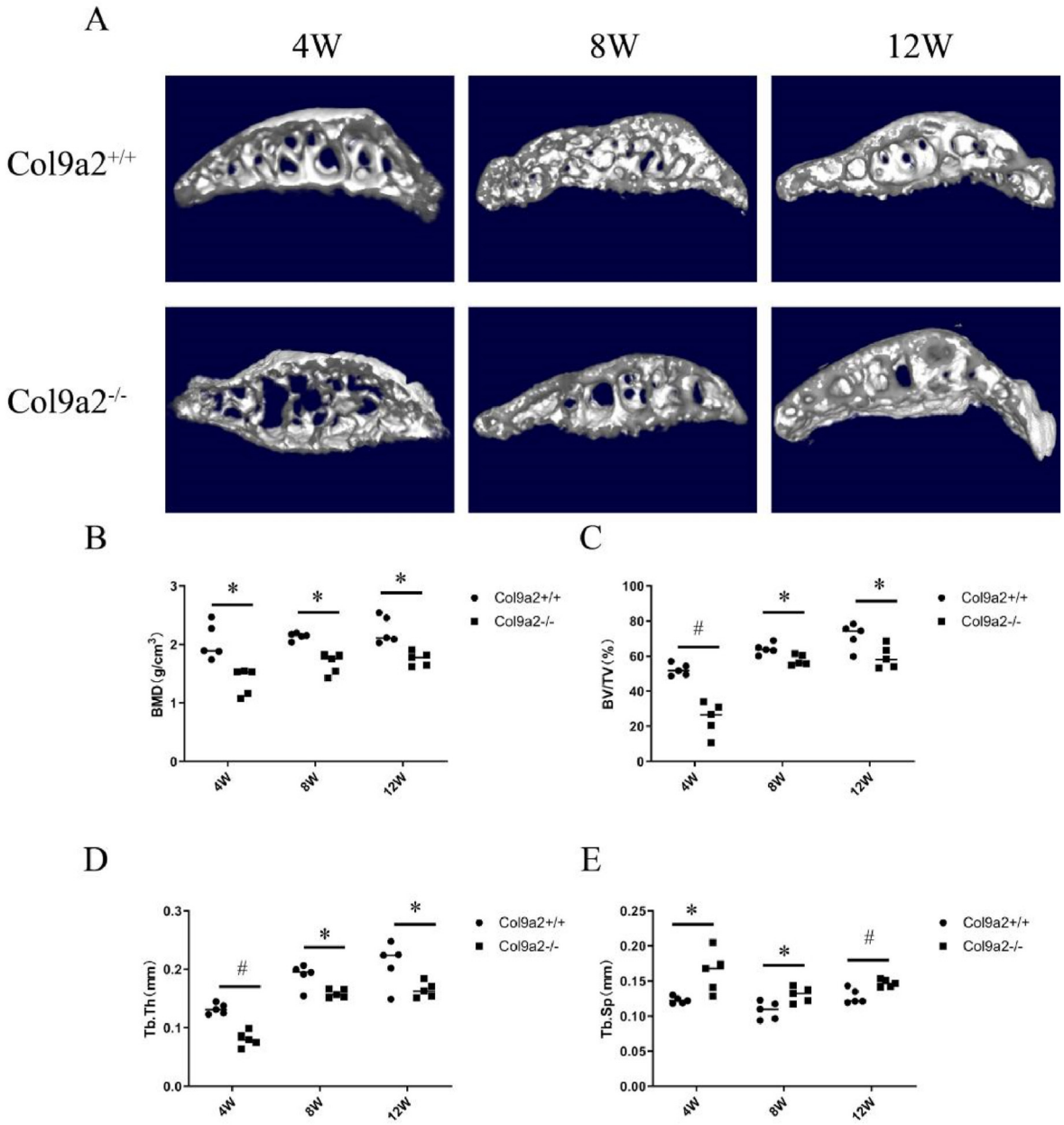

Figure 2. Image and morphometric analysis of μCT of early-stage Col9a2$^{-/-}$ mice. A 3D reconstruction of the subchondral bone of the knee joint. B-E Morphometric analysis of μCT, including BMD (B); BV/TV (C); Tb.Th (D); and Tb.Sp (E). All data were expressed as mean ± SD, $^{*}P < 0.05$, $^{\#}P < 0.01$.

(Col9a2$^{+/+}$) littermates were applied for all experiments. All animals were housed in constant temperature (22 °C) and humidity (40 ± 5%), pathogen-free room, exposed to a controlled light/dark cycle (12h/12 h) with solid rodent chow and water ad libitum. All studies were approved by the Committee on the Ethics of Animal Experiments of Zhejiang Chinese Medical University (Hangzhou, China; approval no. 20190401-10).

2.2. Whole-mount skeletal staining

Skeletal staining of E18.5 and P28 mice were performed with 0.03% Alcian blue (Sigma–Aldrich, A5533) and 0.005% Alizarin red (Sigma–Aldrich, A3157) solutions [16]. These samples were hyalinized in a graded sequence of glycerol and potassium hydroxide and finally stored in 100% glycerol at 4 °C for imaging on a C-DSD230 stereomicroscope (Nikon, Japan).

2.3. Tissue sample and blood sample preparation

All mice were sacrificed at specific time points and the knee joint samples were surgically harvested; specimens were fixed in 4% paraformaldehyde for 48 h, decalcified in 14% EDTA solution (pH = 7.4) for approximately 14 days, then dehydrated and embedded in paraffin, stored at room temperature for further use.

The arterial blood of mice was collected by ophthalmectomy. EP tubes containing blood samples were left at room temperature for 30min, centrifuged at 3000 rpm/min for 15 min at 4 °C, the serum was isolated and stored at −80 °C pending use.

2.4. Micro-CT analysis (μCT)

The representative radiographic images of the knee joint samples were collected by micro-CT equipment (Skyscan 1176, Bruker, Kontich, Belgium). Briefly, the samples were scanned for approximately 400 slices

at a resolution of 9 μm. The region of interest (ROI) was defined between the proximal tibia growth plate and the tibial plateau, and the three-dimensional (3D) structure and ROI of the knee joint samples were reconstructed by using NRecon software (Bruker, Belgium). Several indexes were evaluated as follow: (1) bone mineral density (BMD, g/cm^3); (2) bone volume fraction (BV/TV, %); (3) average trabecular thickness (Tb.Th, mm); (4) average trabecular separation (Tb.Sp, mm).

2.5. Mechanical test

To test the load-bearing capacity of the proximal tibia metaphysis of the samples, static loading was applied to the tibial plateau at 1 mm/min using an axial compression tester (EnduraTec TestBenchTM system, Bose Corp., Minnetonka, MN, USA). Subsequently, the appearance of the first mechanical turning point which attributed to specimen deformation, was defined as load-bearing capacity.

2.6. Histochemistry and histomorphometry

Paraffin-embedded samples were cut into 3 μm sagittal sections as described previously [17]. After deparaffinized in xylene and dehydrated in a series of graded ethanol, the sections were stained with Toluidine Blue and imaged on a light microscope (Axio Scope A1, ZEISS, Germany). The area and thickness of cartilage were calculated using OsteoMeasure Software (OsteoMetrics, Inc., Atlanta, GA, United States). Moreover, cartilage degeneration scores were determined by two blinded observers according to Osteoarthritis Research Society International (OARSI) scoring system as described previously [18].

2.7. Tartrate-resistant acid phosphatase (TRAP) staining

After deparaffinized in xylene and dehydrated in a series of graded ethanol, the sections were subjected to TRAP staining and counterstained with hematoxylin and imaged on a light microscope (Axio Scope A1, ZEISS, Germany), and the number of osteoclasts (N.Oc/T.A) was quantified as previously [19].

2.8. Immunohistochemistry (IHC) and immunofluorescence (IF)

After endogenous peroxidase reduction, antigen retrieve and non-specific background elimination, sections were treated with anti-Col9a2 (diluted 1:100, Santa Cruz, sc398130, USA), anti-Col2 (diluted 1:1000, Millipore, mab1330, USA), anti-Runx2 (diluted 1:200, Abcam, ab76956, UK), anti-Mmp13(diluted 1:200, Abcam, ab39012, UK), anti-Col10 (diluted 1:1000, Abcam, ab58632, UK), anti-ALP (diluted 1:200, arigo, ARG57422, Taiwan, China), anti-Adamts5 (diluted 1:1000, Novus, NB100-74350, USA) primary antibody incubated overnight at 4 °C. For IHC staining, the next day, positive staining was detected with diaminobenzidine (DAB) solution (ZSGB-bio, ZLI-9017, Beijing, China) after reacting with secondary goat anti-mouse/rabbit antibody (diluted 1:1000, Invitrogen, 31234, USA) for 20 min at room temperature, while counterstaining was performed with hematoxylin. Positive staining was detected using a light microscope (Axioscope A1; Zeiss, ZEISS, Germany). For IF staining, the sections were incubated with fluorophore-conjugated secondary antibody at room temperature for 20 min without the light, and then the sections were counterstained with DAPI and observed under a fluorescence microscope (Carl Zeiss AG). Finally, images were quantitatively analyzed by Image-Pro Plus 6.0 (Media Cybernetics, Rockville, Maryland, USA).

2.9. Enzyme linked immunosorbent (Elisa) assay

Serum concentrations of bone turnover markers β-isomerized C-terminal telopeptides (β-CTX) and Procollagen Type I intact N-terminal Propeptide (PINP) were determined using an Elisa kits according to manufacturer's procedures (Jiancheng bioengineering, H285 and H287, Nanjing, China). The absorbance readings were made at 450 nm using a spectrophotometer (BioTek ELx800), and the concentrations of samples were calculated from the standard curve.

2.10. Statistical analysis

All data were described as mean ± SD. One-way ANOVA test and independent-samples t-test, which was used in the present research, were performed using SPSS software (version 24.0, IBM Corporation, NY,

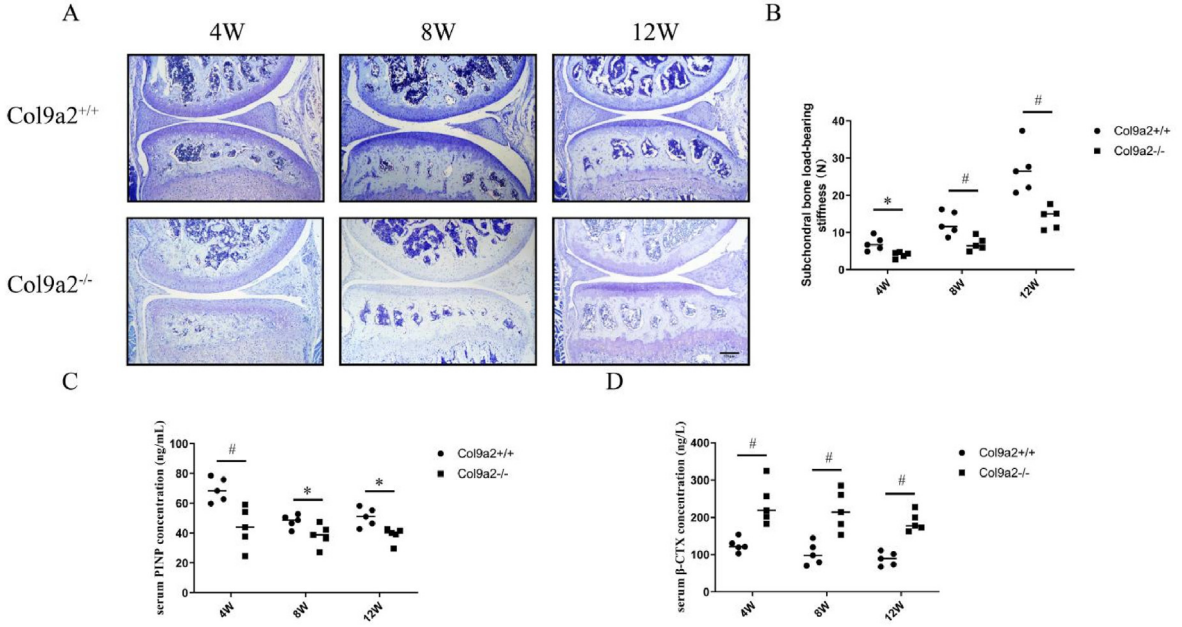

Figure 3. Histopathological, biomechanical and serological changes of early-stage Col9a2$^{-/-}$ mice. A Toluidine blue staining. Scale bar: 100 μm. B Load-bearing capacity of the proximal tibia metaphysis. C,D Serum concentrations of β-CTX (C) and PINP (D). All data were expressed as mean ± SD, $^{*}P < 0.05$, $^{\#}P < 0.01$. (For interpretation of the references to color in this figure legend, the reader is referred to the Web version of this article.)

USA). $P < 0.05$ was considered to be statistically significant (*), meanwhile $P < 0.01$ was classified as highly significant (#).

3. Results

3.1. Col9a2 depletion showed no difference in skeleton morphology in mice

Theoretically, the expression of Col9a2 protein may decrease sharply after Col9a2 gene depletion. As shown in Fig. 1A, Col9a2 if immunofluorescence appeared that the protein was mainly expressed in articular cartilage and the medullary cavity of subchondral bone (SCB), the expression content of SCB was relatively higher. As we expected, the expression of Col9a2 was significantly decreased in Col9a2$^{-/-}$ mice. To figure out whether Col9a2 deficiency could interfere with the skeleton development in mice, we then conducted whole-mount skeletal staining by using embryos (E18.5) and adult mice (P28). The results displayed no difference in bone length and ossification between knockout and Col9a2$^{+/+}$ mice at mid-gestation and adult stages (Fig. 1B).

Col9a2 deficiency disrupts the homeostasis of subchondral bone by activating osteoclasts and inhibiting osteoblasts.

Even though, as mentioned, there were no differences in skeletal appearance between the two types of mice, we wanted to find out if there were any clues to abnormalities in the microstructure of the skeleton. As shown in Figs. 2A and 3D reconstruction analysis of μCT scanning exhibited that the microstructure of the tibial plateau SCB in Col9a2$^{-/-}$ mice was thinner and sparser than that of Col9a2$^{+/+}$ mice at 4w, 8w and 12w. Morphometric analysis of μCT data showed that BMD, BV/TV and Tb.Th were significantly lower in the corresponding regions of the Col9a2$^{-/-}$ mice at 4w, 8w and 12w compared to Col9a2$^{+/+}$ mice (Fig. 2B–D), whereas Tb.Sp was considerably higher (Fig. 2E).

To further explain these findings, we then discuss them by histopathology, biomechanics and serology. Toluidine blue staining manifested that the articular cartilage of Col9a2$^{-/-}$ mice had fewer proteoglycans at 4w, 8w and 12w, although there was no apparent change in thickness. Notably, the SCB of Col9a2$^{-/-}$ mice was considerably deformed compared to Col9a2$^{+/+}$ mice (Fig. 3A). To clarify whether these changes could affect the mechanical properties of the SCB, we examined the load-bearing capacity of the proximal tibial metaphysis. As expected, specimens from Col9a2$^{-/-}$ mice were more prone to deformation under the same mechanical loading (Fig. 3B). PINP and β-CTX are important reference indicators for evaluating osteogenesis and bone resorption, respectively, and in agreement with the imaging results, Col9a2$^{-/-}$ mice also down-regulated serum PINP concentration and up-regulated serum β-CTX concentration (Fig. 3C and D), reflecting the possibility of reduced osteogenesis and increased bone resorption in Col9a2$^{-/-}$ mice. To verify this hypothesis, we then performed TRAP staining and IHC for

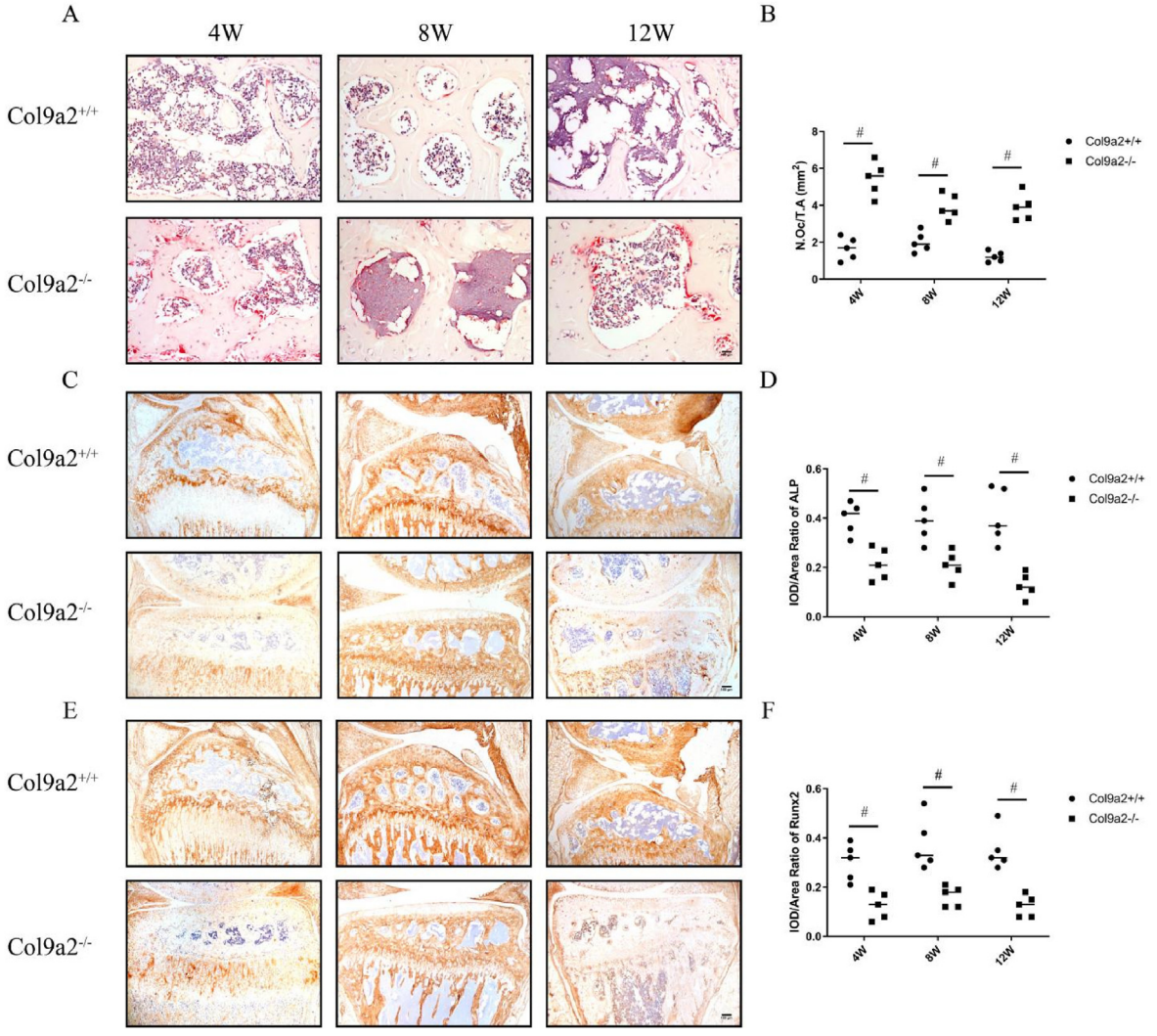

Figure 4. TRAP staining and IHC for osteogenic-related proteins of early-stage Col9a2$^{-/-}$ mice. A,B TRAP staining (A) and osteoclastometric analysis (B). C,D IHC (C) and quantitative analysis (D) of ALP. E,F IHC (E) and quantitative analysis (F) of Runx2. Scale bar: 100 μm. All data were expressed as mean ± SD, *$P < 0.05$, #$P < 0.01$.

osteogenesis-related proteins (ALP and Runx2), which demonstrated that Col9a2$^{-/-}$ mice had a dramatically higher capacity for bone resorption compared to Col9a2$^{+/+}$ mice, as well as a remarkably lower capacity for osteogenesis (Fig. 4A–F).

Col9a2 depletion led to early articular cartilage degeneration and finally caused osteoarthritis-like articular cartilage damage.

Articular cartilage and SCB seem like a functional unit, the underlying bone plate is highly vascularized and provide nutrition for upper hyaline cartilage. We believe that when SCB goes abnormal, cartilage can't stay out of it. To testify our hypothesis, we conducted further studies.

As we described above, in addition to significant deformation of the SCB, there was a reduction in proteoglycans compared to Col9a2$^{+/+}$ mice, although there was no marked change in articular cartilage thickness in Col9a2$^{-/-}$ mice at 4w, 8w and 12w (Fig. 3A). To explain the changes identified by histology, we performed IHC. IHC of the major components of the cartilage matrix (Col2 and Aggrecan) illustrated the expression of both proteins in the ECM of cartilage was dramatically reduced in the Col9a2$^{-/-}$ mice compared to Col9a2$^{+/+}$ mice (Fig. 5A–D), in other words, the cartilage in Col9a2$^{-/-}$ mice degraded faster. Since cartilage anabolism and catabolism are tightly linked, we then performed IHC on proteins related to cartilage catabolism. Among the chondrolysis-related proteins, Col10 is involved in the terminal differentiation of chondrocytes, Adamts5 is responsible for the degradation of Aggrecan, and Mmp13 is capable of degrading Col2 in the cartilage matrix. Surprisingly, whether Col10, Adamts5 or Mmp13, the expression of these proteins was substantially increased in Col9a2$^{-/-}$ mice compared to Col9a2$^{+/+}$ mice, demonstrating ECM degradation (Fig. 6A–F). These results insisted that Col9a2 deficiency could interfere with cartilage ECM anabolism and catabolism.

Based on the imbalance in osteochondral homeostasis in Col9a2$^{-/-}$ mice, we hypothesized that Col9a2 deficiency would eventually cause the destruction of articular cartilage. To examine this hypothesis, we extended the observation time to 36w. Toluidine blue staining revealed that at 24w of age, the Col9a2$^{-/-}$ mice exhibited a marked narrowing of the joint space, reduced cartilage matrix staining and pronounced SCB sclerosis compared to Col9a2$^{+/+}$ mice. At 36w of age, the knee joint degeneration in Col9a2$^{-/-}$ mice was further aggravated with severe cartilage destruction, particularly on the tibial side, and the sclerosis of SCB was further exacerbated (Fig. 7A). Bone morphometrics demonstrated that both the cartilage thickness and area of the tibial plateau were dramatically lower than in the Col9a2$^{+/+}$ mice (Fig. 7B and C). The OARSI of the knee joint was markedly higher in Col9a2$^{-/-}$ mice than in the Col9a2$^{+/+}$ mice (Fig. 7D). The results of the 3D reconstruction analysis of μCT scans further confirmed the degeneration of the knee joint. 24 and 36 week old Col9a2$^{-/-}$ knockout mice displayed distinct osteophytes growth with joint space narrowing compared to Col9a2$^{+/+}$ mice (Fig. 7E). However, morphometric analysis of μCT data showed no significant differences in BV/TV, Tb.Th and Tb.Sp parameters (Fig. 7F–H).

4. Discussion

The progressive degeneration of joints inevitably occurs over the course of a lifetime as a consequence of natural aging or external damage. These are the major risk factors for the progression to osteoarthritis (OA), the most common degenerative bone and joint disease affecting approximately 250 million people worldwide [20–22]. The joint consists primarily of cartilage and SCB, separated by an osteochondral interface, which comprises the deeply packed cartilage and the underlying SCB. These individual components collaborate with each other to form a complex functional unit [23]. Anatomically, the articular cartilage is attached to the SCB, which is a richly vascularized tissue that provides nutrients and material exchange to the hyaline cartilage above [24]. Biomechanically, the stability and integrity of the articular cartilage are dependent on its interaction with the SCB [25], which provides mechanical support to the overlying articular cartilage during weight-bearing joint movements and is in a constant process of deformation and remodeling in order to adapt to the changing mechanical environment [26]. Thus, osteochondral homeostasis is essential for the maintenance of knee joint movement and function.

The collagen plays a pivotal role in osteochondral homeostasis, which provides the structural support for bone and cartilage, and their normal

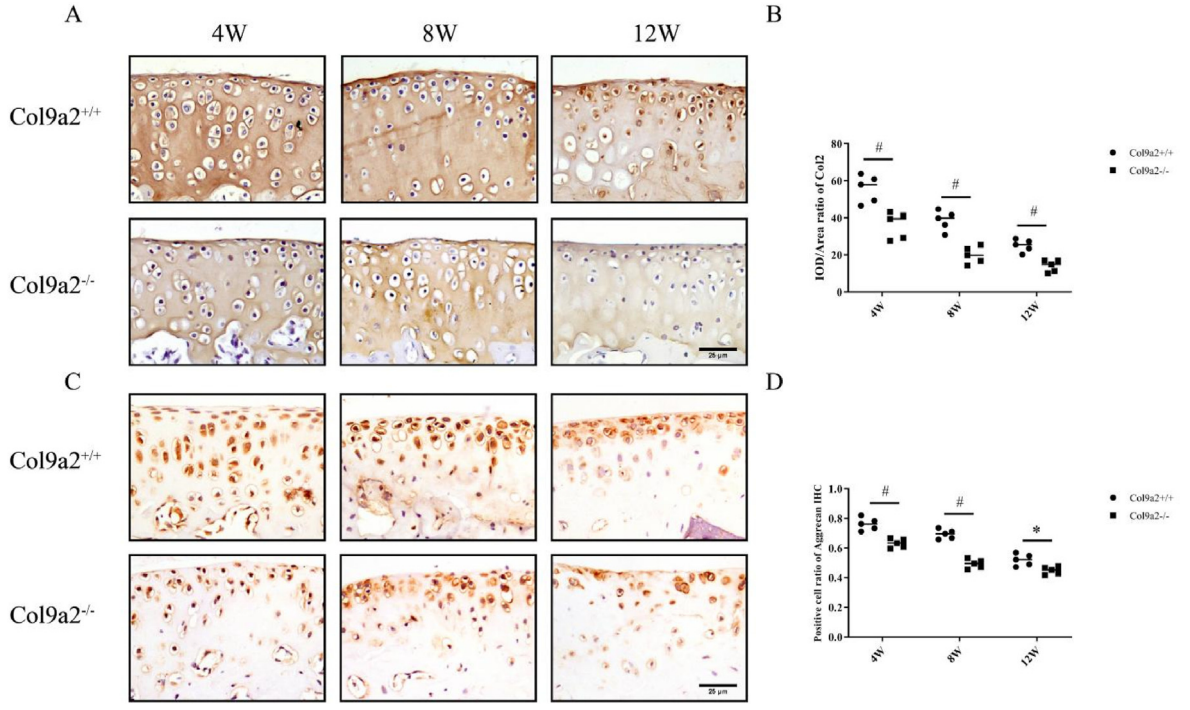

Figure 5. IHC of cartilage ECM anabolic-related proteins of early-stage Col9a2$^{-/-}$ mice. A,B IHC (A) and quantitative analysis (B) of Col2. C,D IHC (C) and quantitative analysis (D) of Aggrecan. Scale bar: 25 μm. All data were expressed as mean ± SD, $^{*}P < 0.05$, $^{\#}P < 0.01$.

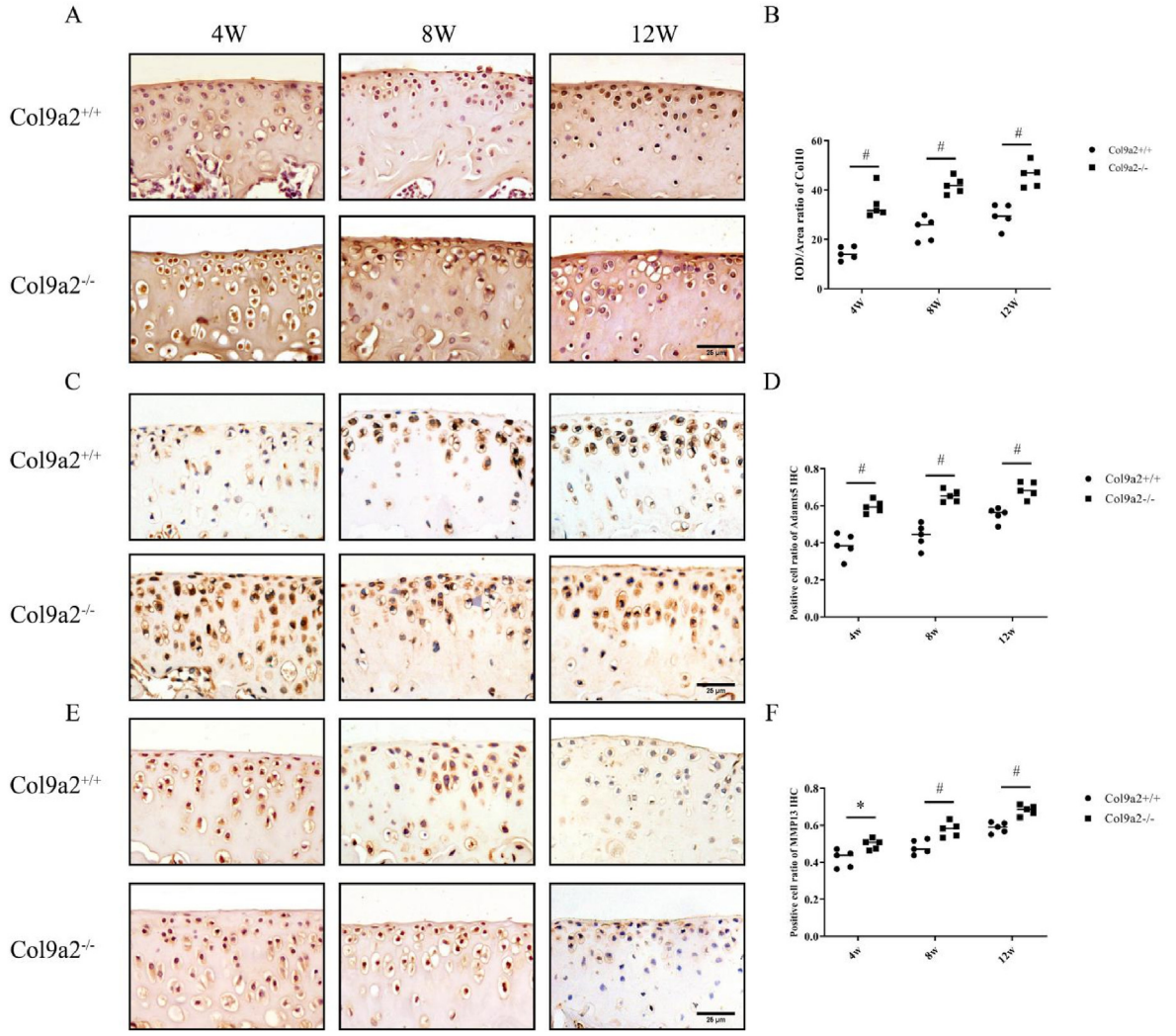

Figure 6. IHC of cartilage ECM catabolic-related proteins of early-stage Col9a2$^{-/-}$ mice. A,B IHC (A) and quantitative analysis (B) of Col10. C,D IHC (C) and quantitative analysis (D) of Adamts5. E,F IHC (E) and quantitative analysis (F) of Mmp13. Scale bar: 25 μm. All data were expressed as mean ± SD, $^{*}P < 0.05$, $^{\#}P < 0.01$.

distribution in time and space ensures the normal morphology of bone and cartilage and their stable biomechanical properties such as resistance to compression and rotation [27]. Col9, together with Col2, forms the scaffold for the ECM in cartilage and is an important component of the collagen network within cartilage [28]. As one of the branched chains of Col9, Col9a2 has been shown to be associated with orthopedic conditions such as intervertebral disc degeneration and multiple epiphyseal dysplasia [6,8–11], but the relationship with OA remains to be elucidated. In the present study, we first demonstrated by whole skeleton staining that the absence of Col9a2 could not affect skeletal development in mice. We then focused on the knee joint to observe the effect of Col9a2 deletion on osteochondral homeostasis. As expected, μCT results revealed remarkable changes in the microstructure and trabecular parameters of the tibial plateau SCB in early Col9a2$^{-/-}$ mice compared to wild-type mice, which were confirmed by pathological staining and biomechanical tests. Bone homeostasis is a state in which bone resorption and bone formation are in a dynamic balance [29,30]. Based on the marked alterations in SCB, we speculated that this might be due to an imbalance in bone homeostasis. Fortunately, Elisa, TRAP staining and IHC results displayed that Col9a2$^{-/-}$ mice exhibited active osteoclastic function, whereas osteogenic function was reduced.

However, the degeneration of the cartilage apparently lagged behind the SCB, with no change in cartilage thickness, except for a decrease in proteoglycan, suggesting that the SCB in Col9a2$^{-/-}$ mice were drastically altered than the cartilage in the early stages. Based on the strong association of SCB with cartilage, it is reasonable to assume that cartilage is altered in addition to a reduction in proteoglycan. IHC results demonstrated that Col9a2 deficiency interferes with the anabolic and catabolic metabolism of cartilage ECM, leading to later cartilage degeneration. Given this striking phenomenon, we are interested in further observing the effect of the absence of Col9a2 on osteochondral homeostasis of the knee joint at a later stage. μCT and pathological staining revealed that in addition to further subchondral osteosclerosis, the Col9a2$^{-/-}$ mice had severely damaged cartilage with highly uneven surfaces, marked fissures and remarkably increased osteophytes growth and joint space narrowing compared to wild-type mice, as well as notably higher OARSI scores. It has been shown that the SCB absorbs most of the biomechanical forces transmitted from the articular surfaces and provides biomechanical support to the cartilage due to its relatively higher stiffness and strength than the overlying cartilage [31]. The decreased capacity of SCB to dissipate loading stresses is expected to alter the stress distribution in articular cartilage, which is detrimental to the maintenance of cartilage homeostasis. Consequently, alterations in the microstructural and biomechanical properties of the SCB inevitably affect its ability to dissipate biomechanical stimuli from the articular surface and subsequently lead to damage to the articular cartilage [32,33]. Furthermore,

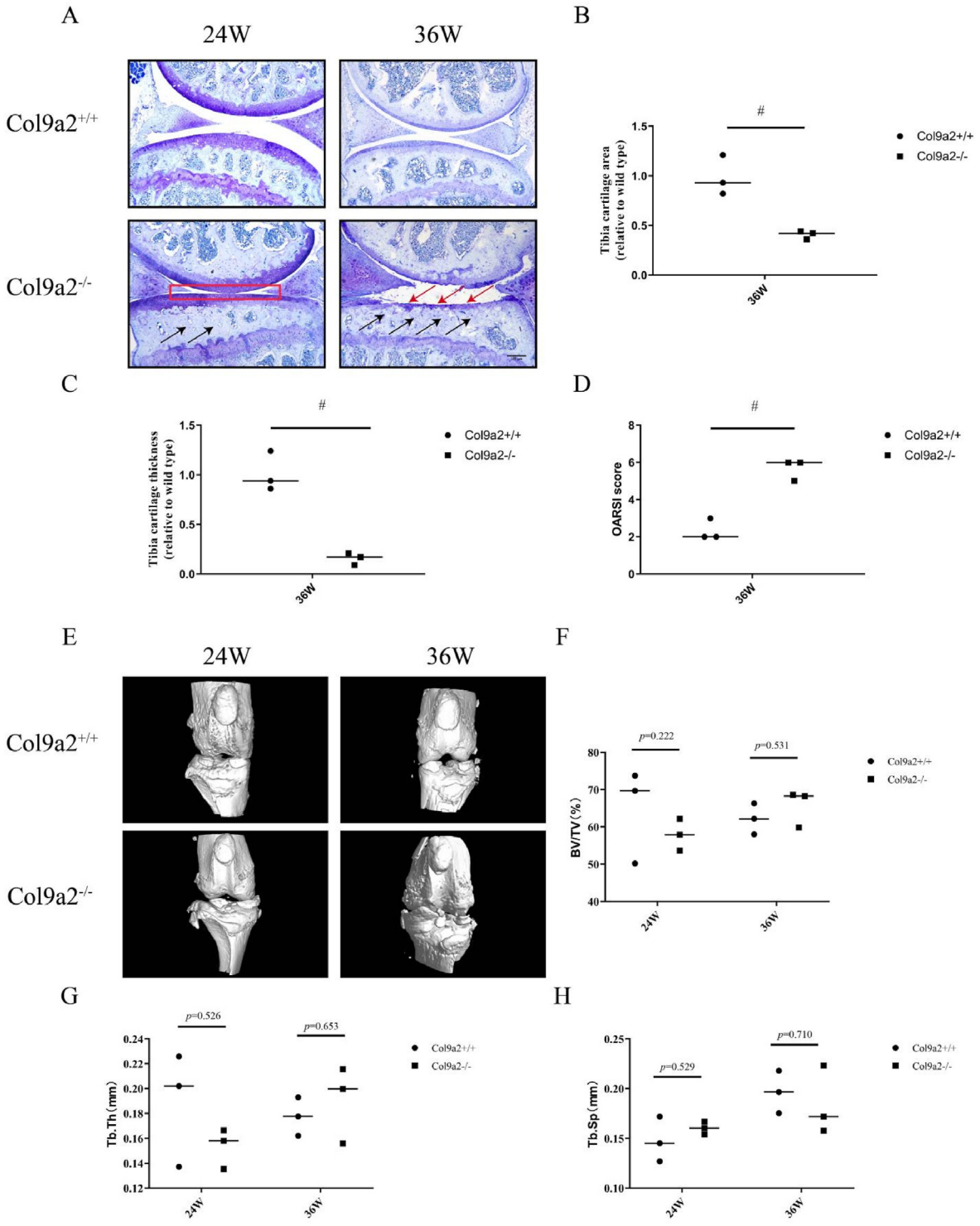

Figure 7. Histopathological staining and μCT analysis of late-stage Col9a2$^{-/-}$ mice. A Toluidine blue staining. Red box indicates the narrowed joint space, black arrows indicate the area of subchondral osteosclerosis and red arrows indicate the area of cartilage defects. Scale bar: 100 μm. B,C Cartilage thickness (B) and area (C) of the tibial plateau. D OARSI score. E 3D reconstruction of the knee joint. F–H Morphometric analysis of μCT, including BV/TV (F); Tb.Th (G) and Tb.Sp (H). All data were expressed as mean ± SD, $^{\#}P < 0.01$. (For interpretation of the references to color in this figure legend, the reader is referred to the Web version of this article.)

the abnormal microstructural and biomechanical properties of cartilage are induced by the abnormal activity of the osteoblasts and osteoclasts of the SCB [34]. However, surprisingly, the morphometric analysis of μCT indicated that there was no significant difference between the two groups of mice in terms of BMD, BV/TV, Tb.Th and Tb.Sp. We speculate that this result may be due to the early onset of osteogenesis and osteoclastic activity of Col9a2 deletion, resulting in sparse bone trabeculae and reduced BMD in the SCB of the knee, although osteoarthritic-like changes in the knee were observed later, it was not at the same level as in wild-type mice and therefore was not comparable in the later stages. Therefore, the lack of statistical significance of the relevant parameters is not sufficient to negate the fact of sclerosis. We considered that while SCB could not provide adequate mechanical support leading to cartilage degeneration in the early stage, the body physiologically accelerated SCB

remodeling trying to strengthen SCB and improve the biomechanical bearing capacity of SCB. Therefore, when the phenotype of knee osteoarthritis appeared in the late stage, The SCB, due to the loss of original bone mass, did not exhibit a more severe degree of sclerosis than the wild type, but a comparable amount of bone mass.

5. Conclusion

In conclusion, Col9a2 is essential for the maintenance of osteochondral homeostasis in the knee joint of mice. After the knockout of this gene, the sclerosis of SCB is dramatically accompanied by the reduction of load-bearing capacity; in the late stages, excessive load is continuously applied to the cartilage in the presence of SCB stress depression, ultimately causing osteoarthritis-like articular cartilage damage.

Contributions

L Xiao, S Lv, P Tong and H Jin conceived of the studies and planned the experimental design. R Dong, H Xu, P Wang, L Fang performed the experiments and analyzed the data. H Xu wrote the manuscript, R Dong assisted with data interpretation and performed critical revisions on the manuscript. All authors approved the final manuscript.

Funding

This research has been partially supported by the Natural Science Foundation of China (Grant nos. 82274280 and 82004389), Zhejiang grants funded by Provincial Natural Science Foundation of China (Grant No. LD22C060002 and LR23H270001), the State Administration of Traditional Chinese Medicine of Zhejiang Province (Grant nos. 2021ZZ014 and 2023ZR018).

Declaration of AI and AI-assisted technologies in the writing process

The authors declare never used of AI and AI assisted technologies during writing process.

Declaration of competing interest

The authors declare no conflict of interest relevant to this article.

Acknowledgements

We appreciate the great help/technical support/experimental support from the Public Platform of Medical Research Center, Academy of Chinese Medical Science, Zhejiang Chinese Medical University.

References

[1] Paassilta P, Pihlajamaa T, Annunen S, Brewton RG, Wood BM, Johnson CC, et al. Complete sequence of the 23-kilobase human COL9A3 gene. Detection of Gly-X-Y triplet deletions that represent neutral variants. J Biol Chem 1999;274(32):22469–75.
[2] Pihlajamaa T, Vuoristo MM, Annunen S, Perala M, Prockop DJ, Ala-Kokko L. Human COL9A1 and COL9A2 genes. Two genes of 90 and 15 kb code for similar polypeptides of the same collagen molecule. Matrix Biol 1998;17(3):237–41.
[3] Eyre DR, Pietka T, Weis MA, Wu JJ. Covalent cross-linking of the NC1 domain of collagen type IX to collagen type II in cartilage. J Biol Chem 2004;279(4):2568–74.
[4] Bruckner P. Suprastructures of extracellular matrices: paradigms of functions controlled by aggregates rather than molecules. Cell Tissue Res 2010;339(1):7–18.
[5] Roberts S, Menage J, Duance V, Wotton S, Ayad S. Volvo Award in basic sciences. Collagen types around the cells of the intervertebral disc and cartilage end plate: an immunolocalization study. Spine 1991;16(9):1030–8. 1991.
[6] Hyun SJ, Park BG, Rhim SC, Bae CW, Lee JK, Roh SW, et al. A haplotype at the COL9A2 gene locus contributes to the genetic risk for lumbar spinal stenosis in the Korean population. Spine 2011;36(16):1273–8.
[7] Xu H, Dong R, Zeng Q, Fang L, Ge Q, Xia C, et al. Col9a2 gene deletion accelerates the degeneration of intervertebral discs. Exp Ther Med 2022;23(3):207.
[8] Annunen S, Paassilta P, Lohiniva J, Perala M, Pihlajamaa T, Karppinen J, et al. An allele of COL9A2 associated with intervertebral disc disease. Science 1999;285(5426):409–12.
[9] Jim JJ, Noponen-Hietala N, Cheung KM, Ott J, Karppinen J, Sahraravand A, et al. The TRP2 allele of COL9A2 is an age-dependent risk factor for the development and severity of intervertebral disc degeneration. Spine 2005;30(24):2735–42.
[10] Aladin DM, Cheung KM, Chan D, Yee AF, Jim JJ, Luk KD, et al. Expression of the Trp2 allele of COL9A2 is associated with alterations in the mechanical properties of human intervertebral discs. Spine 2007;32(25):2820–6.
[11] Noponen-Hietala N, Kyllonen E, Mannikko M, Ilkko E, Karppinen J, Ott J, et al. Sequence variations in the collagen IX and XI genes are associated with degenerative lumbar spinal stenosis. Ann Rheum Dis 2003;62(12):1208–14.
[12] Nakki A, Videman T, Kujala UM, Suhonen M, Mannikko M, Peltonen L, et al. Candidate gene association study of magnetic resonance imaging-based hip osteoarthritis (OA): evidence for COL9A2 gene as a common predisposing factor for hip OA and lumbar disc degeneration. J Rheumatol 2011;38(4):747–52.
[13] Spayde EC, Joshi AP, Wilcox WR, Briggs M, Cohn DH, Olsen BR. Exon skipping mutation in the COL9A2 gene in a family with multiple epiphyseal dysplasia. Matrix Biol 2000;19(2):121–8.
[14] Muragaki Y, Mariman EC, van Beersum SE, Perala M, van Mourik JB, Warman ML, et al. A mutation in COL9A2 causes multiple epiphyseal dysplasia (EDM2). Ann N Y Acad Sci 1996;785:303–6.
[15] Zhang R, Guo H, Yang X, Li Z, Zhang D, Li B, et al. Potential candidate biomarkers associated with osteoarthritis: evidence from a comprehensive network and pathway analysis. J Cell Physiol 2019;234(10):17433–43.
[16] Rigueur D, Lyons KM. Whole-mount skeletal staining. Methods Mol Biol 2014;1130:113–21.
[17] Xu HH, Li SM, Fang L, Xia CJ, Zhang P, Xu R, et al. Platelet-rich plasma promotes bone formation, restrains adipogenesis and accelerates vascularization to relieve steroids-induced osteonecrosis of the femoral head. Platelets 2021;32:950–9.
[18] Xu HH, Li SM, Xu R, Fang L, Xu H, Tong PJ. Predication of the underlying mechanism of Bushenhuoxue formula acting on knee osteoarthritis via network pharmacology-based analyses combined with experimental validation. J Ethnopharmacol 2020;263:113217.
[19] Zhang P, Xu H, Wang P, Dong R, Xia C, Shi Z, et al. Yougui pills exert osteoprotective effects on rabbit steroid-related osteonecrosis of the femoral head by activating beta-catenin. Biomed Pharmacother 2019;120:109520.
[20] Felson DT, Niu J, Yang T, Torner J, Lewis CE, Aliabadi P, et al. Physical activity, alignment and knee osteoarthritis: data from MOST and the OAI. Osteoarthritis Cartilage 2013;21(6):789–95.
[21] Sanchez-Adams J, Leddy HA, McNulty AL, O'Conor CJ, Guilak F. The mechanobiology of articular cartilage: bearing the burden of osteoarthritis. Curr Rheumatol Rep 2014;16(10):451.
[22] Hunter DJ, Bierma-Zeinstra S. Osteoarthritis. Lancet 2019;393(10182):1745–59.
[23] Yuan XL, Meng HY, Wang YC, Peng J, Guo QY, Wang AY, et al. Bone-cartilage interface crosstalk in osteoarthritis: potential pathways and future therapeutic strategies. Osteoarthritis Cartilage 2014;22(8):1077–89.
[24] Imhof H, Sulzbacher I, Grampp S, Czerny C, Youssefzadeh S, Kainberger F. Subchondral bone and cartilage disease: a rediscovered functional unit. Invest Radiol 2000;35(10):581–8.
[25] Lories RJ, Luyten FP. The bone-cartilage unit in osteoarthritis. Nat Rev Rheumatol 2011;7(1):43–9.
[26] Madry H, van Dijk CN, Mueller-Gerbl M. The basic science of the subchondral bone. Knee Surg Sports Traumatol Arthrosc 2010;18(4):419–33.
[27] Ott SM. Bone strength: more than just bone density. Kidney Int 2016;89(1):16–9.
[28] Wu JJ, Woods PE, Eyre DR. Identification of cross-linking sites in bovine cartilage type IX collagen reveals an antiparallel type II-type IX molecular relationship and type IX to type IX bonding. J Biol Chem 1992;267(32):23007–14.
[29] Nakahama K. Cellular communications in bone homeostasis and repair. Cell Mol Life Sci 2010;67(23):4001–9.
[30] Eriksen EF. Cellular mechanisms of bone remodeling. Rev Endocr Metab Disord 2010;11(4):219–27.
[31] Zhen G, Cao X. Targeting TGFbeta signaling in subchondral bone and articular cartilage homeostasis. Trends Pharmacol Sci 2014;35(5):227–36.
[32] Goldring SR. Alterations in periarticular bone and cross talk between subchondral bone and articular cartilage in osteoarthritis. Ther Adv Musculoskelet Dis 2012;4(4):249–58.
[33] Intema F, Hazewinkel HA, Gouwens D, Bijlsma JW, Weinans H, Lafeber FP, et al. In early OA, thinning of the subchondral plate is directly related to cartilage damage: results from a canine ACLT-meniscectomy model. Osteoarthritis Cartilage 2010;18(5):691–8.
[34] Chu L, Liu X, He Z, Han X, Yan M, Qu X, et al. Articular cartilage degradation and aberrant subchondral bone remodeling in patients with osteoarthritis and osteoporosis. J Bone Miner Res 2020;35(3):505–15.